Fig 1. Representative images showing SWI stages according to the number of conspicuous DMVs draining into the subependymal veins: stage 1, mild (<5; A); stage 2, moderate (5–10; B); and stage 3, severe (>10, namely "brush like"; C).

Patient characteristics in each presentation of MMD

	Asymptomatic	TIA	Infarct	Hemorrhage	P
N	4	13	9	7	
Age, yr	19 ± 9.5	27 ± 18.3	33 ± 14.5	37 ± 21.0	.31
Suzuki stage	3 ± 0.0	3.3 ± 0.5	3.1 ± 0.3	3 ± 0.0	.37
CBF					
MCA	52.3 ± 26.8	39.7 ± 8.3	33.4 ± 10.6	47.8 ± 20.1	.2
Basal ganglia	54.1 ± 19.8	44.7 ± 8.0	45.9 ± 13.9	37.7 ± 5.0	.32
Thalamus	52.7 ± 13.8	43.7 ± 7.1	42.0 ± 12.6	38.9 ± 4.3	.3
CVR					
MCA	38.29 ± 5.6	2.49 ± 21.0*	−2.16 ± 14.5*	13.1 ± 20.0	.02
Basal ganglia	59.3 ± 0.0	13.04 ± 20.4*	14.07 ± 8.5*	22.17 ± 14.2	.03
Thalamus	70.47 ± 0.0	32.89 ± 17.1*	21.8 ± 7.6**	26.4 ± 10.4*	.006

*$P < 0.05$, **$P < 0.01$.

1 than stages 2 and 3 in the cortical MCA area ($P < .05$; Fig 3A) compared with in the basal ganglia (Fig 3C) and thalamus (Fig 3E). In contrast, CVR was significantly lower in SWI stage 3 in the cortical MCA area ($P < .05$; Fig 3B), and a similar trend was seen in the basal ganglia (Fig 3D) and thalamus (Fig 3F).

Images from cases from the study are shown in Fig 4.

Discussion

This is the first report showing characteristics of the DMV in MMD by using SWI techniques. Susceptibility-weighted MR imaging is a high spatial resolution 3D gradient-echo MR imaging technique with phase postprocessing that accentuates the paramagnetic properties of blood products such as deoxy-hemoglobin, intracellular methemoglobin, and hemosid-erin.[10] This technique can show prominent hypointense signals in the draining veins within areas of impaired perfusion. Uncoupling between oxygen supply and demand in hypoperfused tissue may cause a relative increase of deoxyhemoglobin levels and a decrease of oxyhemoglobin in the tissue capillaries and the draining veins. Therefore, SWI has been applied to various pathologies of the brain that affect magnetic inhomogeneity, such as stroke,[8,11] trauma,[8] cerebral cavernous malformation,[12,13] arteriovenous malformation,[14] dural arteriovenous fistula,[15] pathophysiology affecting iron storage conditions,[16-18] brain tumor,[19] and cerebral amyloid angiopathy.[20] It is noteworthy that this method has the potential to demonstrate increased oxygen extraction in focal cerebral ischemia.[8]
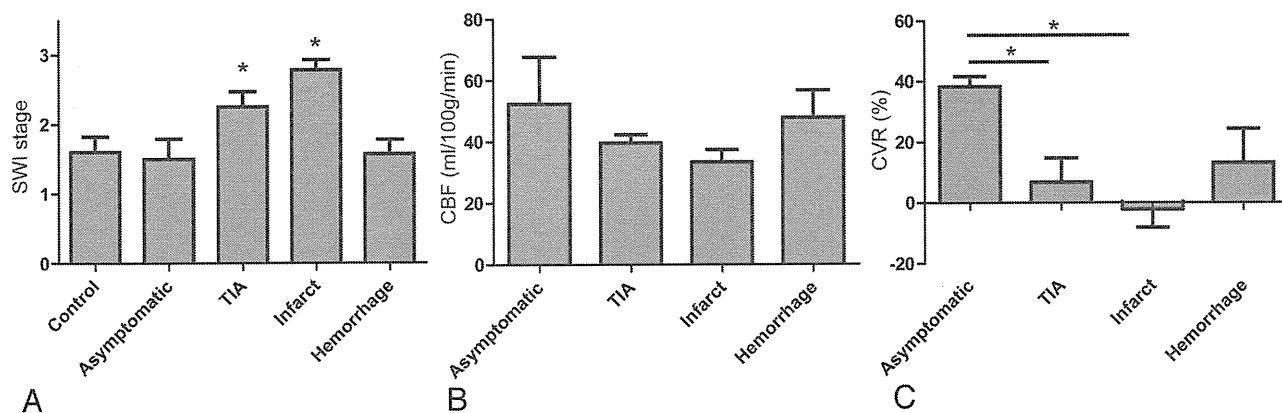
Fig 2. SWI staging (A), CBF (B), and CVR (C) in each presentation type of MMD. *P < .05.
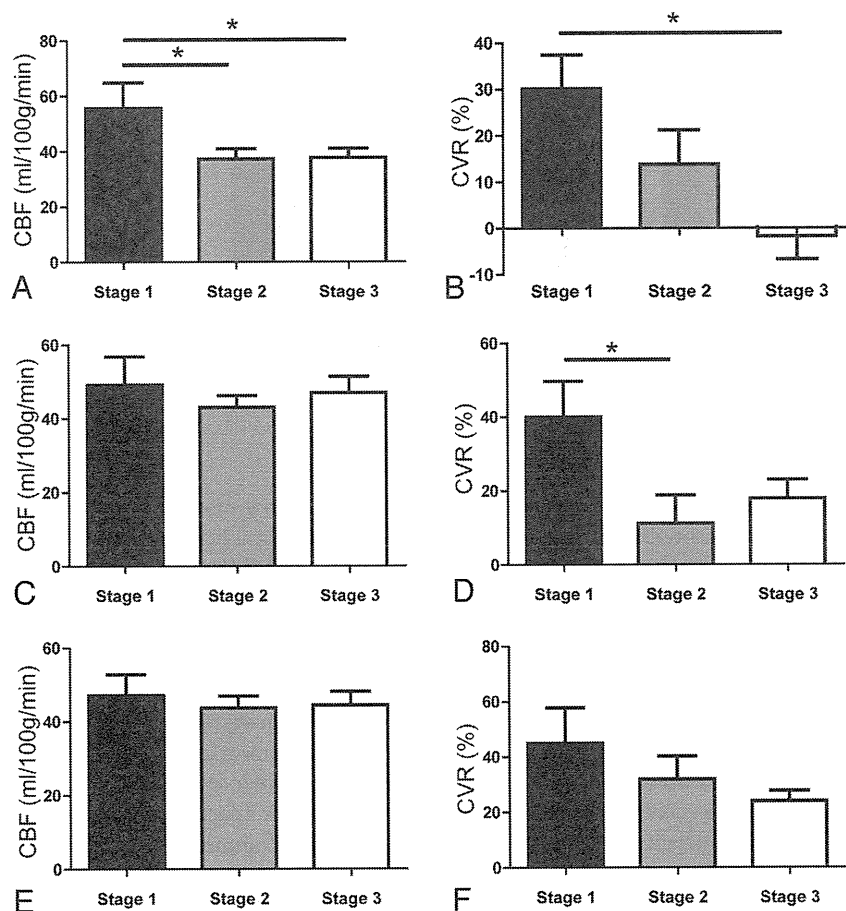

Fig 3. CBF (A, C, and E) and CVR (B, D, and F) in each SWI stage. The region of interest was located in the cortical MCA area (A and B), basal ganglia (C and D), and thalamus (E and F). *P < .05.

In MMD, increased conspicuity of DMVs was found in patients with TIA and infarct, implying that impaired perfusion occurred in the deep white matter. This result supports the specification that conspicuous DMVs indicate increased oxygen extraction or venous stasis, and this indicates a part of misery perfusion in this area.[8,21] Susceptibility-weighted MR imaging shows prominent hypointense signals in the draining veins within areas of impaired perfusion. Therefore, this would account for the increased visibility of veins in these regions, making it valuable to anticipate the extent of impaired perfusion in MMD without contrast-enhanced CT or MR im-

aging, SPECT, or PET. Alternatively, DSC-weighted bolus tracking MR imaging and ASL are the latest additions to the growing number of techniques available for quantitative hemodynamic analysis.[5] ASL is becoming more clinically relevant for evaluating CBF because this method has other advantages, including lack of radiation, lack of intravenous contrast agent, and the ability to repeat the study. In terms of MMD, however, the delayed arterial times through collateral pathways can cause a significant underestimation of CBF as well as errors due to labeling agent that remains in the feeding vessels rather than being extracted into the brain parenchyma.[4]
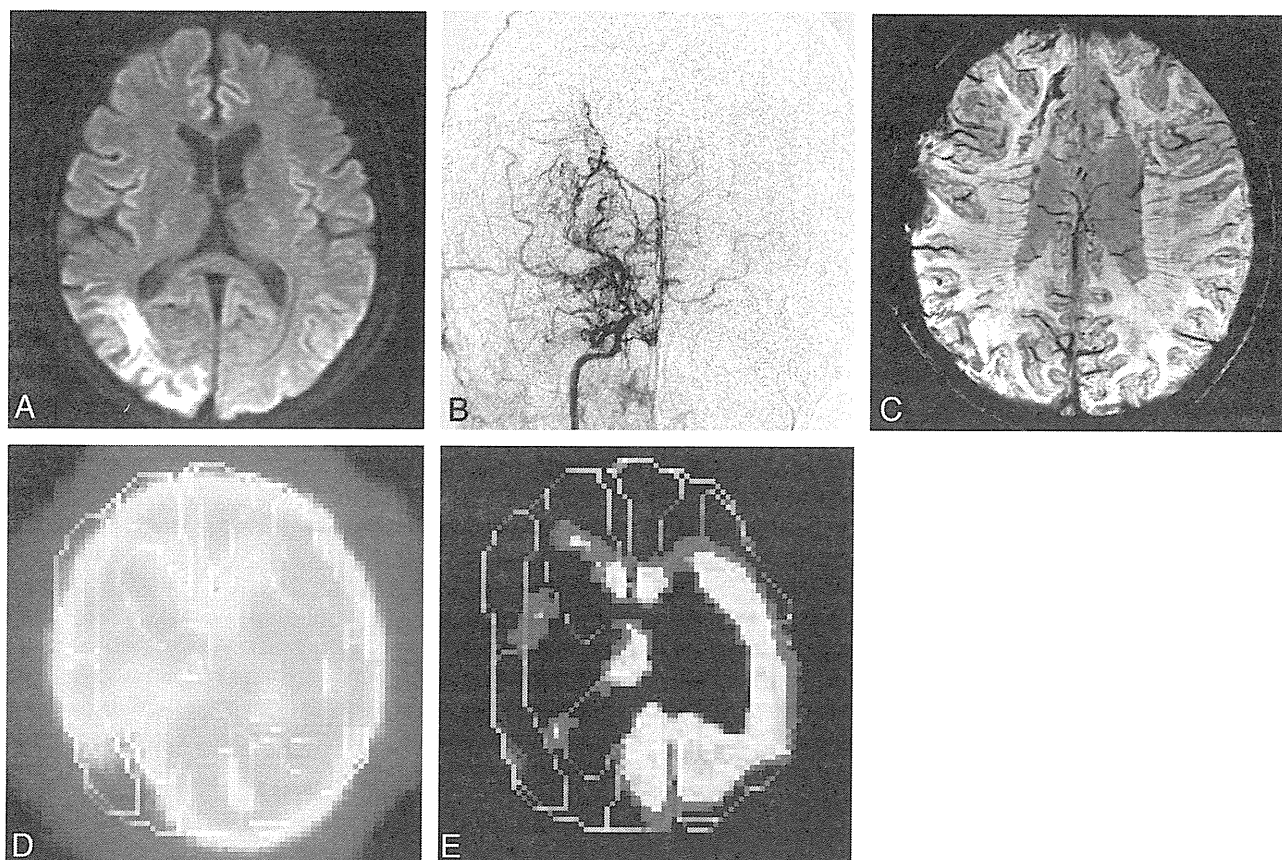
79

Fig 4. *A,* 37-year-old man showing infarction in the right occipital lobe. *B,* Intra-arterial angiography showing Suzuki stage 3 MMD. Brush signs can be seen in the deep white matter on SWI *(C)* with low CBF *(D)* and CVR *(E)* on SPECT.

Moreover, patients with MMD are in a chronic state of cerebral vasodilation and have a reduced or absent CVR. Therefore, CVR is also a valuable hemodynamic indicator in MMD, though there have been no MR imaging techniques reported for the assessment of CVR so far. Here, we first show SWI could correlate with hemodynamics in SPECT, especially CVR.

Another interesting finding in this study is that SWI stage and CBF and CVR were not so impaired in patients presenting with hemorrhage compared with those presenting with TIA or infarct. Intracranial hemorrhage is a common in feature in adult patients with MMDs with a mortality rate of approximately 20%, and it is the largest risk factor contributing to the poor prognosis with this entity.[22,23] Hemodynamic stress to the Moyamoya vessels has been suggested as a cause for the hemorrhagic presentation, and some reports showed Moyamoya vessels and aneurysms associated with MMD resolved after bypass surgery.[24,25] The prophylactic effect of bypass surgery against cerebral hemorrhage remains uncertain, and this issue will be clarified by a prospective, randomized trial in Japan (Japan Adult Moyamoya Trial). Here, we showed severe hemodynamic compromise was not obvious in the hemorrhagic group. Although there is less consensus regarding the hemodynamic findings in hemorrhagic MMD, some supportive reports have so far shown that CBF in MMD is not significantly lower in any presentations and that there is a significant difference in CBV and OEF between the patients with ischemia and hemorrhage, with a higher CBV and increased OEF

(lower CVR) in the ischemic group.[26,27] Moreover, the disturbances in cerebral hemodynamics are usually less prominent in adults with MMD than in pediatric patients.[28,29] Together, this suggests that hemodynamic impairment does not always contribute to the hemorrhagic presentation, which is common in adults.

The SWI technique also can detect MBs, reported to be a predictor for hemorrhage in MMD.[30] MBs were detected in 18.8% (3 in hemorrhage groups and 3 in TIA groups) in our series. The incidence of MBs is reported as 14.8%–42%, depending on MR imaging quality such as 1.5T versus 3T or T2* versus SWI technique.[31-33] The significance of MBs in patients with an ischemic presentation is still controversial. Kikuta et al[32] reported MBs occurred with equal probability regardless of the MMD onset type (44% in hemorrhage versus 43% in ischemia). In contrast, Ishikawa et al[33] reported that patients with hemorrhage had more MBs than those with ischemia (33.3% in hemorrhage versus 11.1% in ischemia). Initially, the characteristic clinical feature of MMD suggests that a patient could have both ischemic and hemorrhagic stroke, and 13% of patients with MMD with hemorrhage have experienced ischemic attacks before admission.[34] Further study is necessary to determine whether MBs are specific for a hemorrhagic presentation.

Several limitations in this study should be addressed. First, this study was performed as a preoperative study and did not interpret SWI data for decision making for revascularization surgery. Second, we could not characterize the signal intensity

change of the DMV on SWI after revascularization surgery. Therefore, the utility of SWI to predict whether a patient with MMD would benefit from bypass surgery is still not clear. In our institute, the main indication for revascularization surgery was symptomatic MMD and asymptomatic MMD with impaired hemodynamics (lower CBF and CVR) when evaluated by SPECT. Direct and indirect combined bypass surgery (STA-MCA anastomosis with encephalomyosynangiosis) was mainly performed for the patients with MMD, and indirect bypass surgery (encephalo-duro-arterio-synangiosis) was selected in case the STA was not developed. In this study, direct and indirect combined bypass was performed in 17 patients, indirect bypass was performed in 3 patients, and 13 patients were treated conservatively. More data should be accumulated by using SWI to address these limitations. Third, this study was not a quantitative analysis and SWI could not replace other modalities for the assessment of the cerebral hemodynamics. Nevertheless, SWI could be a simple and powerful technique to assess CVR in MMD without acetazolamide challenges.

Conclusions

In this study, we found that SWI stage strongly correlates with ischemic MMD and also correlates with hemodynamics in SPECT, especially CVR. Increased conspicuity of DMVs known as "brush sign" with SWI could predict the severity of MMD.

References

1. Suzuki J, Takaku A. Cerebrovascular "Moyamoya" disease. Disease showing abnormal net-like vessels in base of brain. Arch Neurol 1969;20:288–99
2. Suzuki J, Kodama N. Moyamoya disease—a review. Stroke 1983;14:104–09
3. Kuroda S, Houkin K. Moyamoya disease: current concepts and future perspectives. Lancet Neurol 2008;7:1056–66
4. Lee M, Zaharchuk G, Guzman R, et al. Quantitative hemodynamic studies in Moyamoya disease: a review. Neurosurg Focus 2009;26:E5
5. Tanaka Y, Nariai T, Nagaoka T, et al. Quantitative evaluation of cerebral hemodynamics in patients with Moyamoya disease by dynamic susceptibility contrast magnetic resonance imaging—comparison with positron emission tomography. J Cereb Blood Flow Metab 2006;26:291–300
6. Honda M, Ezaki Y, Kitagawa N, et al. Quantification of the regional cerebral blood flow and vascular reserve in Moyamoya disease using split-dose iodoamphetamine I 123 single-photon emission computed tomography. Surg Neurol 2006;66:155–59
7. Imaizumi M, Kitagawa K, Hashikawa K, et al. Detection of misery perfusion with split-dose 123I-iodoamphetamine single-photon emission computed tomography in patients with carotid occlusive diseases. Stroke 2002;33:2217–23
8. Tong KA, Ashwal S, Obenaus A, et al. Susceptibility-weighted MR imaging: a review of clinical applications in children. AJNR Am J Neuroradiol 2008;29:9–17
9. Fukui M. Guidelines for the diagnosis and treatment of spontaneous occlusion of the circle of Willis ('Moyamoya' disease). Research Committee on Spontaneous Occlusion of the Circle of Willis (Moyamoya Disease) of the Ministry of Health and Welfare, Japan. Clin Neurol Neurosurg 1997;99 Suppl 2:S238–40
10. Sehgal V, Delproposto Z, Haacke EM, et al. Clinical applications of neuroimaging with susceptibility-weighted imaging. J Magn Reson Imaging 2005;22:439–50
11. Wycliffe ND, Choe J, Holshouser B, et al. Reliability in detection of hemor-

rhage in acute stroke by a new three-dimensional gradient recalled echo susceptibility-weighted imaging technique compared to computed tomography: a retrospective study. J Magn Reson Imaging 2004;20:372–77
12. Lee BC, Vo KD, Kido DK, et al. MR high-resolution blood oxygenation level-dependent venography of occult (low-flow) vascular lesions. AJNR Am J Neuroradiol 1999;20:1239–42
13. Reichenbach JR, Jonetz-Mentzel L, Fitzek C, et al. High-resolution blood oxygen-level dependent MR venography (HRBV): a new technique. Neuroradiology 2001;43:364–69
14. Essig M, Reichenbach JR, Schad LR, et al. High-resolution MR venography of cerebral arteriovenous malformations. Magn Reson Imaging 1999;17:1417–25
15. Noguchi K, Kuwayama N, Kubo M, et al. Intracranial dural arteriovenous fistula with retrograde cortical venous drainage: use of susceptibility-weighted imaging in combination with dynamic susceptibility contrast imaging. AJNR Am J Neuroradiol 2010;31:1903–10
16. Bartzokis G, Tishler TA. MRI evaluation of basal ganglia ferritin iron and neurotoxicity in Alzheimer's and Huntington's disease. Cell Mol Biol (Noisy-le-grand) 2000;46:821–33
17. Bartzokis G, Cummings JL, Markham CH, et al. MRI evaluation of brain iron in earlier- and later-onset Parkinson's disease and normal subjects. Magn Reson Imaging 1999;17:213–22
18. Hecht MJ, Fellner C, Schmid A, et al. Cortical T2 signal shortening in amyotrophic lateral sclerosis is not due to iron deposits. Neuroradiology 2005;47:805–08
19. Sehgal V, Delproposto Z, Haddar D, et al. Susceptibility-weighted imaging to visualize blood products and improve tumor contrast in the study of brain masses. J Magn Reson Imaging 2006;24:41–51
20. Greenberg SM, O'Donnell HC, Schaefer PW, et al. MRI detection of new hemorrhages: potential marker of progression in cerebral amyloid angiopathy. Neurology 1999;53:1135–38
21. Tamura H, Hatazawa J, Toyoshima H, et al. Detection of deoxygenation-related signal change in acute ischemic stroke patients by T2*-weighted magnetic resonance imaging. Stroke 2002;33:967–71
22. Kobayashi E, Saeki N, Oishi H, et al. Long-term natural history of hemorrhagic Moyamoya disease in 42 patients. J Neurosurg 2000;93:976–80
23. Kawaguchi S, Okuno S, Sakaki T. Effect of direct arterial bypass on the prevention of future stroke in patients with the hemorrhagic variety of Moyamoya disease. J Neurosurg 2000;93:397–401
24. Kuroda S, Houkin K, Ishikawa T, et al. Novel bypass surgery for Moyamoya disease using pericranial flap: its impacts on cerebral hemodynamics and long-term outcome. Neurosurgery 2010;66:1093–101
25. Kuroda S, Houkin K, Kamiyama H, et al. Effects of surgical revascularization on peripheral artery aneurysms in Moyamoya disease: report of three cases. Neurosurgery 2001;49:463–67
26. Nariai T, Matsushima Y, Imae S, et al. Severe haemodynamic stress in selected subtypes of patients with Moyamoya disease: a positron emission tomography study. J Neurol Neurosurg Psychiatry 2005;76:663–69
27. Piao R, Oku N, Kitagawa K, et al. Cerebral hemodynamics and metabolism in adult Moyamoya disease: comparison of angiographic collateral circulation. Ann Nucl Med 2004;18:115–21
28. Kuwabara Y, Ichiya Y, Otsuka M, et al. Cerebral hemodynamic change in the child and the adult with Moyamoya disease. Stroke 1990;21:272–77
29. Kuwabara Y, Ichiya Y, Sasaki M, et al. Cerebral hemodynamics and metabolism in Moyamoya disease—a positron emission tomography study. Clin Neurol Neurosurg 1997;99 Suppl 2:S74–78
30. Kikuta K, Takagi Y, Nozaki K, et al. Histological analysis of microbleed after surgical resection in a patient with Moyamoya disease. Neurol Med Chir (Tokyo) 2007;47:564–67
31. Mori N, Miki Y, Kikuta K, et al. Microbleeds in Moyamoya disease: susceptibility-weighted imaging versus T2*-weighted imaging at 3 Tesla. Invest Radiol 2008;43:574–79
32. Kikuta K, Takagi Y, Nozaki K, et al. Asymptomatic microbleeds in Moyamoya disease: T2*-weighted gradient-echo magnetic resonance imaging study. J Neurosurg 2005;102:470–75
33. Ishikawa T, Kuroda S, Nakayama N, et al. Prevalence of asymptomatic microbleeds in patients with Moyamoya disease. Neurol Med Chir (Tokyo) 2005;45:495–500
34. Fujii K, Ikezaki K, Irikura K, et al. The efficacy of bypass surgery for the patients with hemorrhagic Moyamoya disease. Clin Neurol Neurosurg 1997;99 Suppl 2:S194–95

81

INTERNAL MEDICINE

Cerebral Microbleeds in Patients with Moyamoya-like Vessels Secondary to Atherosclerosis

Makiko Tanaka, Manabu Sakaguchi, Kaori Miwa and Kazuo Kitagawa

Abstract

Objective Hemorrhagic risk is unknown in patients with moyamoya-like vessels associated with atherosclerotic intracranial cerebral artery occlusion. This study was undertaken to investigate the association between moyamoya-like vessels and cerebral microbleeds (CMBs) in patients with atherosclerotic steno-occlusive disease.

Methods The study population comprised 34 patients with steno-occlusive lesions in the intracranial cerebral artery caused by atherosclerosis. We evaluated the presence of moyamoya-like vessels at the base of the brain by cerebral angiography, and the presence of CMBs by T2*-weighted MRI. Patients were divided into 2 groups: those with and those without moyamoya-like vessels; clinical histories and the incidence of CMBs were compared between the groups.

Results Sixteen patients had moyamoya-like vessels. Twelve of 16 patients with moyamoya-like vessels had a history of ischemic stroke or transient ischemic attack, whereas only 1 patient had a history of symptomatic cerebral hemorrhage. The incidence of CMBs did not differ between the 2 groups (31% vs. 28%, p=0.82). The location of CMBs varied and was not associated with the site of moyamoya-like vessels.

Conclusion CMBs were not associated with moyamoya-like vessels in patients with atherosclerotic cerebral artery occlusion. These patients may not have a high risk of cerebral hemorrhage.

Key words: atherosclerosis, cerebral microbleeds, moyamoya phenomenon, magnetic resonance imaging, intracranial hemorrhage

Introduction

Moyamoya disease is characterized by chronic, progressive, bilateral stenosis of the terminal portion of the internal carotid arteries or its proximal branches, with no known cause, and it leads to the formation of an abnormal vascular network composed of collateral pathways (moyamoya vessels) at the base of the brain (1, 2). In adult patients, moyamoya disease frequently manifests with sudden-onset intracranial hemorrhage (3, 4). Hemorrhage is assumed to be the result of the collapse of fragile moyamoya vessels by hemodynamic loading and rupture of the peripheral aneurysms that are often formed on moyamoya vessels (5). Several studies showed that the incidence of cerebral microbleeds (CMBs) in adult patients with moyamoya disease, as detected by gradient-recalled echo (GRE) T2*-weighted magnetic resonance imaging (MRI), is higher than that in healthy individuals, indicating that multiple CMBs are a predictor of subsequent hemorrhage in these patients (6-8).

Moyamoya-like vessels, which also mean abnormal vascular networks at the base of the brain, are associated with cerebrovascular steno-occlusive disease caused by atherosclerosis and this condition is distinguished from moyamoya disease (9-11). The risk of intracranial hemorrhage in patients with moyamoya-like vessels secondary to atherosclerosis is unknown, although these patients frequently receive antithrombotic agents. The aim of this study was to investigate the association between basal moyamoya-like vessels and CMBs in patients with intracranial cerebral artery occlusion by atherosclerosis.

Table 1.   Clinical History of the Patients (n=34)

Age (years), mean ± SD	61.4 ± 11.1
Sex (M/F, N)	22/12
Hypertension, N	29
Diabetes, N	13
Dyslipidemia, N	27
Current smoking, N	9
Stroke or TIA, N	27
Occlusive vascular lesion	
Middle cerebral artery	29
Anterior cerebral artery	8
Carotid siphon	6

TIA; transient ischemic attack

Materials and Methods

Patients

In all, 62 patients with intracranial steno-occlusive arteries, and with less than 50% stenosis in the extracranial carotid arteries, underwent cerebral digital subtraction angiography for clinical assessment of the cerebral artery, between March 2000 and June 2010 at our department. All patients had 1 or more intracranial arterial stenosis≥75% or occlusion. T2*-weighted GRE MRI data were available for 51 of the 62 patients. Given our focus on moyamoya phenomenon caused by atherosclerosis, we excluded patients with cerebrovascular occlusion of unknown origin, including patients with moyamoya disease or suspected moyamoya disease (n= 12), patients with cerebral angiitis (n=1), and patients with other autoimmune disease (n=2). Patients who had undergone extracranial-to-intracranial arterial bypass surgery (n= 2) were also excluded. The remaining 34 patients (22 men and 12 women, 38-74 years old) were included in the study. The cause of the intracranial stenosis or occlusion was clinically presumed to be atherosclerotic in all patients, based on the clinical manifestation, the presence of atherosclerotic cerebrovascular changes in other areas, and 1 or more atherosclerotic risk factors. Most of the patients had steno-occlusive lesions in the stem of the middle cerebral artery (Table 1); some patients had more than 1 steno-occlusive lesion. The study group included 27 symptomatic and 7 asymptomatic patients. The symptomatic patients had a history of transient ischemic attack (n=8), minor ischemic stroke (n=18), or intracranial hemorrhage (n=1). In the asymptomatic patients, including those who had non-focal symptoms such as dizziness or headache, the stenotic lesions were detected incidentally by MR angiography. We evaluated their angiographic and MRI data, and their clinical histories. All study protocols were approved by the Ethics Committee for Clinical Research in our institute.

Imaging

All patients underwent digital subtraction angiography for clinical purposes. Angiographic information included the site of steno-occlusive lesion and the presence of moyamoya-like vessels on the side of the occluded artery (Fig. 1). The presence of moyamoya-like vessels at the base of the brain was assessed by 2 investigators in the arterial phase images.

All MR examinations were performed on a 1.5 T imager (Signa, GE Healthcare, Milwaukee, WI) with a commercially available head coil. The subject was supine, with the neck and head in the neutral position. Axial T2*-weighted GRE sequences were obtained (repetition time / echo time, 600 / 20 ms; flip angle, 20°; matrix, 256×256; field of view, 220 mm; slice thickness, 5 mm). At the same time, axial T 1-weighted sequences and axial T2-weighted sequences were acquired to distinguish CMBs from the signal voids of cerebral arteries and from other mass lesions with hemorrhage, such as cavernous angiomas. Fluid-attenuated inversion recovery sequences were acquired to evaluate subcortical and deep white matter lesions.

CMBs were defined as homogeneous, round, hypointense lesions (<10 mm in diameter) in the brain parenchyma on GRE MRI (12). Macrobleeds were distinguished from microbleeds, i.e., lesions with a diameter of≥10 mm on GRE MRI were distinguished as macrobleeds. Hypointense lesions within the subarachnoid space, and areas of symmetrical hypointensity in the globus pallidus on GRE, were considered to represent adjacent pial blood vessels or calcifications, and were excluded. The presence and location of CMBs were assessed independently by 2 trained observers blinded to all clinical information about the subjects. When results differed between the evaluators, the decision was made after consulting a third evaluator.

Subcortical and deep white-matter lesions were evaluated using a rating scale (0-3) devised by Fazekas et al, and were defined as positive when the white-matter lesions were scored as 2 or 3 (13).

Statistical analyses

All analyses were performed with JMP 8.0.2 (SAS Institute Inc., Cary, NC). Based on the presence or absence of basal moyamoya-like vessels, the patients were classified into 2 groups. The presence of CMBs, presence of white-matter lesions, and clinical histories were compared between the groups. The patients were also divided into 2 groups according to the presence or absence of CMBs, and clinical variables were compared between the groups. We used Mann-Whitney's U test for continuous data and the χ^2 test for categorical data. Fisher's exact test (2-tailed) was used in place of the χ^2 test for categorical data when the number of cells was less than 5. Probability values<0.05 were considered significant.

Results

Of the 34 patients, 16 patients had moyamoya-like vessels. Twelve of 16 (75%) patients with moyamoya-like vessels and 14 of 18 (78%) patients without moyamoya-like vessels had a history of ischemic stroke or transient ischemic attack. Only 1 patient with moyamoya-like vessels had a history of symptomatic cerebral hemorrhage (Table 2).
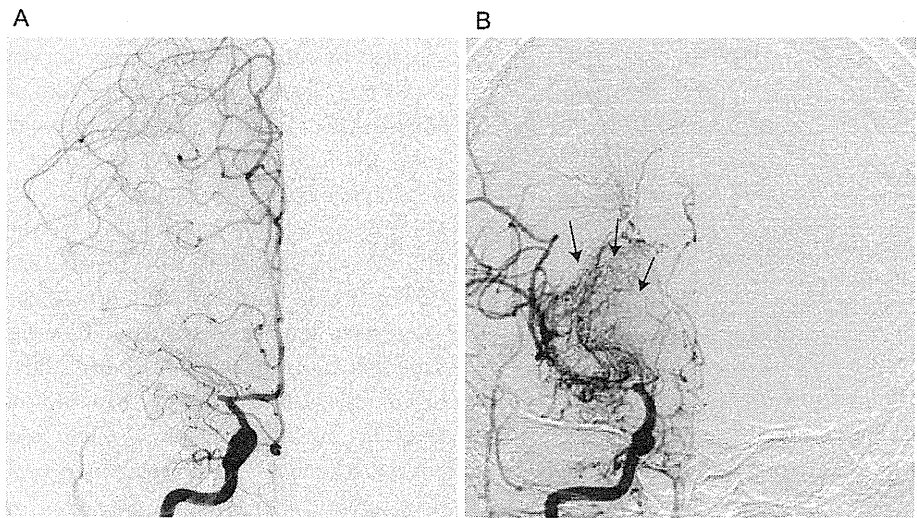
A   B

Figure 1.   Representative angiographic images in patients with and without moyamoya-like ves-
sels. A; anteroposterior image of a patient with right middle cerebral artery occlusion. No apparent
moyamoya-like vessels at the base of the brain are visualized. B; anteroposterior image of a patient
with moyamoya-like vessels. The arrows indicate moyamoya-like vessels at the base of the brain.

Table 2.   Stroke Subtypes of Patients with and without Moyamoya-like
Vessels

	Moyamoya-like vessels (+) n = 16	Moyamoya-like vessels (-) n = 18
Atherothrombotic	6	10
Lacunar	1	1
Transient ischemic attack	5	3
Cerebral hemorrhage	1	0
Asymptomatic	3	4

Table 3.   Clinical Histories of Patients with and without Moy-
amoya-like Vessels

	Moyamoya-like vessels (+) n = 16	Moyamoya-like vessels (-) n = 18	p
N	16	18	
Age (years), mean ± SD	64.2 ± 7.9	58.8 ± 13.0	0.39
Male, %	50.0	77.8	0.09
Cerebral microbleeds, %	31.3	27.8	0.82
Hypertension, %	87.5	83.3	1.00
Diabetes, %	31.3	44.4	0.41
Dyslipidemia, %	87.5	72.2	0.41
Current smoking, %	12.5	38.9	0.13
Ischemic heart disease, %	31.3	5.6	0.08
Stroke or TIA, %	81.3	77.8	1.00
Antithrombotic drugs, %	75.0	83.3	0.68

TIA; transient ischemic attack

Ten patients had CMBs, 1 had asymptomatic cerebral macrobleeds, and 1 had symptomatic bleeding. The incidence of asymptomatic CMBs did not differ between patients with and without moyamoya-like vessels (31% vs. 28%, p=0.82). The patients with moyamoya-like vessels included a higher proportion of women (p=0.09) and patients with ischemic heart disease (p=0.08) (Table 3). Meanwhile, the presence of white-matter lesions appeared to be related to the presence of CMBs. Other clinical factors were not as-

sociated with the presence of CMBs (Table 4).

Table 5 shows the location and number of CMBs or macrobleeds and angiographic findings in each patient. In the group with moyamoya-like vessels, two patients had CMBs located close to the moyamoya-like vessels (Patient 2 and Patient 4) and the others had CMBs away from the moyamoya-like vessels.

Table 4. Variables Relevant to Cerebral Microbleeds

	CMB(+)	CMB(-)	p
N	10	24	
Age	61.7 ± 13.5	61.3 ± 10.3	0.64
Male, %	70.0	62.5	1.00
Hypertension, %	80.0	87.5	0.62
Diabetes, %	50.0	33.3	0.36
Dyslipidemia, %	90.0	75.0	0.64
Current smoking, %	20.0	29.2	0.69
Ischemic heart disease, %	20.0	16.7	1.00
Stroke or TIA, %	80.0	79.2	1.00
Antithrombotic drugs, %	70.0	83.3	0.39
Deep white matter lesion, %	60.0	29.2	0.13
Moyamoya-like vessels, %	50.0	45.8	0.82

CMB, cerebral microbleed; TIA, transient ischemic attack

Table 5. Number and Location of Cerebral Microbleeds/Macrobleeds and Angiographic Findings

No.	Age and sex	Cerebral microbleeds and macrobleeds		Angiographic findings
		Location	Total number	
Moyamoya-like vessels (+)				
1	65 M	Bil thalamus	2	R M1 O, L A2 S, R basal MM
2	70 F	R putamen	1	R M1 O, R A2 S, R basal MM
3	72 M	R temporal subcortex	1	R M1 O, R basal MM
4	73 M	L frontal cortex	1	Bil carotid siphon O, Bil expansive MM
5	69 M	R temporal subcortex	1	L M1 O, L carotid siphon S, L basal MM
6	50 M	R frontal subcortex (30 mm, symptomatic)	1	R M1 O, R basal MM
Moyamoya-like vessels (-)				
7	62 M	L thalamus, L para lateral ventricle	2	L M1 O
8	55 M	Pons, Bil thalamus, putamen, and corona radiata	14	L M1 S, L A1 O
9	74 F	R parieto-occipital subcortex, R thalamus	2	R M1 S
10	58 M	L thalamus, L putamen	3	L M1 S, L A1 S
11	39 F	Bil thalamus	2	L M1 S
12	72 M	L caudate nucleus (15 mm, asymptomatic)	1	L M1 O

M; male, F; female, R; right, L; left, Bil; bilateral, O; occlusion, S; stenosis, MM; moyamoya-like vessels

Discussion

CMBs have a prevalence of 5.7% and are observed more frequently with advancing age (14). The Rotterdam Scan Study determined that the prevalence of CMBs was 17.8% in the general population aged 60-69 years and 38.3% in those over 80 years old (15). The prevalence of CMBs is also much higher in patients with ischemic stroke than in the healthy population (34% vs. 5%) (16). CMBs are particularly associated with hypertensive small vessel diseases. Among the stroke subtypes, the incidence of CMBs is sig-nificantly greater in patients with intracerebral hemorrhage and patients with lacunar infarction than in patients with cardioembolic infarction, patients with atherothrombotic infarction, or healthy individuals (17). The prevalence of CMBs was 29.4% in our subjects. The subjects of the present study had a mean age of 61.4 years, and most had a history of ischemic stroke or transient ischemic attack. The prevalence of CMBs was not high compared to the reported prevalence in elderly patients with ischemic stroke.

CMBs are also detected in patients with adult moyamoya disease. The reported prevalence of CMBs was 15-44% and it varied according to MRI resolution (6, 7). However, the

mean age of those subjects was in the early 40s, indicating that those subjects were much younger than most patients with hypertensive small vessel diseases. According to the histopathological findings, fragile moyamoya vessels were indicated to be the cause of CMBs (18). Moreover, multiple CMBs in adult moyamoya disease were reported to be a risk factor for subsequent intracranial hemorrhage (8). CMBs can be considered a marker for the risk of intracranial hemorrhage in moyamoya disease.

We showed here that CMBs were not associated with the site of basal moyamoya-like vessels caused by atherosclerotic steno-occlusive cerebral arteries, and that the prevalence of CMBs did not differ in patients with moyamoya-like vessels and patients without moyamoya-like vessels. CMBs in our patients were presumed to represent the microangiopathy ordinarily caused by atherosclerosis, and its pathology may not be the same as that of CMBs in adult moyamoya disease.

In our subjects, the history of symptomatic cerebral hemorrhage was scarce, but the prevalence of ischemic events was high. In the previous reports of patients with moyamoya-like vasculopathy from atherosclerotic occlusive disease, most patients presented with cerebral ischemia and cerebral hemorrhage was rare (10, 11, 19-21). Moyamoya-like vessels may be less likely to be associated with the risk of cerebral hemorrhage in atherosclerotic occlusive disease than in adult moyamoya disease. Medical therapies are not effective for moyamoya disease. The frequencies of ischemic and hemorrhagic stroke are both high in adults whose moyamoya disease is treated conservatively (22-24). However, patients with atherosclerotic intracranial occlusive artery should receive antithrombotic treatment on the basis of individual hemorrhagic risks despite the presence of moyamoya-like vessels.

The reason for the differing hemorrhagic risk between adult moyamoya disease and moyamoya phenomenon secondary to atherosclerosis is not clear. Differing features of these 2 diseases are the site of the occlusive major cerebral arteries and the age at onset. Collateral vessels, including extensive moyamoya vessels, develop alongside progressive occlusive changes in the terminal portion of the internal carotid arteries in adult moyamoya disease. Moyamoya phenomenon secondary to atherosclerosis, however, is often associated with occlusion in the intracranial branch vessels, such as the stems of the middle cerebral artery and the anterior cerebral artery without including the internal carotid arteries (25). The extent of the collateral vessels is restricted in these cases. The degree of proliferation of basal moyamoya vessels may therefore be associated with hemorrhagic risk. In addition, the anterior choroidal and posterior communicating arteries are hemodynamically overloaded with occlusion at the terminal portion of the internal carotid artery. Dilatation of the anterior choroidal and posterior communicating arteries is also reported to be a predictor of hemorrhage in adult moyamoya disease (26). Furthermore, moyamoya vessels develop for decades, beginning in childhood, in adult moyamoya disease. The vulnerability of the moyamoya vessels may increase with the passage of time (5).

The present study has several limitations. First, in this small cohort, multivariate analysis was not definitive. CMBs were not associated with known risk factors such as aging and hypertension in the present study, perhaps because of the small number of patients and the fact that most of them had these risk factors. Second, because the present study was cross-sectional, the risk for subsequent cerebral hemorrhage was not clear in patients with moyamoya-like vessels. Prospective data on clinical outcomes for patients with moyamoya-like vessels secondary to atherosclerosis are needed.

Conclusion

The prevalence and site of CMBs did not differ between patients with and without moyamoya-like vessels. Patients with moyamoya-like vessels secondary to atherosclerosis had a high frequency of ischemic cerebrovascular diseases, and slight symptomatic cerebral hemorrhage. Patients with moyamoya-like vessels secondary to atherosclerosis may not have a high risk of cerebral hemorrhage.

The authors state that they have no Conflict of Interest (COI).

References

1. Suzuki J, Takaku A. Cerebrovascular "moyamoya" disease. Disease showing abnormal net-like vessels in base of brain. Arch Neurol 20: 288-299, 1969.
2. Scott RM, Smith ER. Moyamoya disease and moyamoya syndrome. N Engl J Med 360: 1226-1237, 2009.
3. Kuroda S, Ishikawa T, Houkin K, Nanba R, Hokari M, Iwasaki Y. Incidence and clinical features of disease progression in adult moyamoya disease. Stroke 36: 2148-2153, 2005.
4. Kuroda S, Houkin K. Moyamoya disease: current concepts and future perspectives. Lancet Neurol 7: 1056-1066, 2008.
5. Takahashi JC, Miyamoto S. Moyamoya disease: recent progress and outlook. Neurol Med Chir (Tokyo) 50: 824-832, 2010.
6. Ishikawa T, Kuroda S, Nakayama N, Terae S, Kudou K, Iwasaki Y. Prevalence of asymptomatic microbleeds in patients with moyamoya disease. Neurol Med Chir (Tokyo) 45: 495-500; discussion 500, 2005.
7. Kikuta K, Takagi Y, Nozaki K, et al. Asymptomatic microbleeds in moyamoya disease: T2*-weighted gradient-echo magnetic resonance imaging study. J Neurosurg 102: 470-475, 2005.
8. Kikuta K, Takagi Y, Nozaki K, Sawamoto N, Fukuyama H, Hashimoto N. The presence of multiple microbleeds as a predictor of subsequent cerebral hemorrhage in patients with moyamoya disease. Neurosurgery 62: 104-111, 2008.
9. Fukui M. Guidelines for the diagnosis and treatment of spontaneous occlusion of the circle of Willis ('moyamoya' disease). Research Committee on Spontaneous Occlusion of the Circle of Willis (Moyamoya Disease) of the Ministry of Health and Welfare, Japan. Clin Neurol Neurosurg 99 Suppl 2: S238-S240, 1997.

10. Hinshaw DB Jr, Thompson JR, Hasso AN. Adult arteriosclerotic moyamoya. Radiology 118: 633-636, 1976.

11. Ashley WW Jr, Zipfel GJ, Moran CJ, Zheng J, Derdeyn CP. Moyamoya phenomenon secondary to intracranial atherosclerotic disease: diagnosis by 3T magnetic resonance imaging. J Neuroimaging 19: 381-384, 2009.

12. Koennecke HC. Cerebral microbleeds on MRI: prevalence, associations, and potential clinical implications. Neurology 66: 165-171, 2006.

13. Fazekas F, Kleinert R, Roob G, et al. Histopathologic analysis of foci of signal loss on gradient-echo T2*-weighted MR images in patients with spontaneous intracerebral hemorrhage: evidence of microangiopathy-related microbleeds. AJNR Am J Neuroradiol 20: 637-642, 1999.

14. Fiehler J. Cerebral microbleeds: old leaks and new haemorrhages. Int J Stroke 1: 122-130, 2006.

15. Vernooij MW, van der Lugt A, Ikram MA, et al. Prevalence and risk factors of cerebral microbleeds: the Rotterdam Scan Study. Neurology 70: 1208-1214, 2008.

16. Cordonnier C, Al-Shahi Salman R, Wardlaw J. Spontaneous brain microbleeds: systematic review, subgroup analyses and standards for study design and reporting. Brain 130: 1988-2003, 2007.

17. Kato H, Izumiyama M, Izumiyama K, Takahashi A, Itoyama Y. Silent cerebral microbleeds on T2*-weighted MRI: correlation with stroke subtype, stroke recurrence, and leukoaraiosis. Stroke 33: 1536-1540, 2002.

18. Kikuta K, Takagi Y, Nozaki K, Okada T, Hashimoto N. Histological analysis of microbleed after surgical resection in a patient with moyamoya disease. Neurol Med Chir (Tokyo) 47: 564-567, 2007.

19. Kato H, Shimosegawa E, Oku N, et al. Cerebral hemodynamics and oxygen metabolism in patients with moyamoya syndrome associated with atherosclerotic steno-occlusive arterial lesions. Cerebrovasc Dis 26: 9-15, 2008.

20. Steinke W, Tatemichi TK, Mohr JP, Massaro A, Prohovnik I, Solomon RA. Caudate hemorrhage with moyamoya-like vasculopathy from atherosclerotic disease. Stroke 23: 1360-1363, 1992.

21. Sato M, Kohama A, Fukuda A, Tanaka S, Fukunaga M, Morita R. Moyamoya-like diseases associated with ventricular hemorrhages: report of three cases. Neurosurgery 17: 260-266, 1985.

22. Choi JU, Kim DS, Kim EY, Lee KC. Natural history of moyamoya disease: comparison of activity of daily living in surgery and non surgery groups. Clin Neurol Neurosurg 99 Suppl 2: S11-S18, 1997.

23. Kobayashi E, Saeki N, Oishi H, Hirai S, Yamaura A. Long-term natural history of hemorrhagic moyamoya disease in 42 patients. J Neurosurg 93: 976-980, 2000.

24. Hallemeier CL, Rich KM, Grubb RL Jr, et al. Clinical features and outcome in North American adults with moyamoya phenomenon. Stroke 37: 1490-1496, 2006.

25. Tanaka M, Sakaguchi M, Kitagawa K. Mechanism of moyamoya vessels secondary to intracranial atherosclerotic disease: angiographic findings in patients with middle cerebral artery occlusion. J Stroke Cerebrovasc Dis 2010 (Epub ahead of print).

26. Morioka M, Hamada J, Kawano T, et al. Angiographic dilatation and branch extension of the anterior choroidal and posterior communicating arteries are predictors of hemorrhage in adult moyamoya patients. Stroke 34: 90-95, 2003.

Distribution of Moyamoya Disease Susceptibility Polymorphism p.R4810K in RNF213 in East and Southeast Asian Populations

Wanyang LIU,[1] Toshiaki HITOMI,[1] Hatasu KOBAYASHI,[1]
Kouji H. HARADA,[1] and Akio KOIZUMI[1]

[1]Department of Health and Environmental Sciences,
Graduate School of Medicine Kyoto University, Kyoto, Kyoto

Abstract

Moyamoya disease is an idiopathic vascular disorder of the intracranial arteries. *Ring finger 213 (RNF213)* was previously identified as the strongest susceptibility gene for moyamoya disease in East Asian people by a genome-wide linkage analysis and exome analysis. The coding variant p.R4810K in *RNF213* was strongly associated with moyamoya disease in the Japanese (odds ratio: 338.94, p = 1.05 × 10^{-100}) and Korean (odds ratio: 135.63, p = 7.59 × 10^{-27}) populations, and much less strongly associated in the Chinese population (odds ratio: 14.70, p = 2.63 × 10^{-5}). The present study investigated the distribution of variant p.R4810K in *RNF213* in 2,508 participants from East and Southeast Asian countries using a TaqMan probe. p.R4810K was detected at an allele frequency of about 1.00% in 4 of 11 investigated locations in China. In contrast, p.R4810K was detected homogeneously at relatively high frequencies of 1.00–1.72% in all investigated locations in Korea and Japan, including Okinawa. p.R4810K was not detected in Southeast Asian populations. The population susceptible to moyamoya disease was estimated to be 16.16 million people in East Asian countries, including 11.41 million Chinese, 1.36 million Korean, and 3.39 million Japanese people. The number of patients with moyamoya disease, which was estimated at approximately one per 300 carriers of p.R4810K, was considered to be 53,800 in East Asian populations.

Key words: moyamoya disease, p.R4810K, *RNF213*, East Asian, Southeast Asian

Introduction

Moyamoya disease (Mendelian Inheritance in Man [MIM] number 607151) is a rare idiopathic progressive disorder characterized by occlusive lesions in the supraclinoid internal carotid artery and its main branches in the circle of Willis. The reduction in blood flow in the regions affected by the occlusive lesions is compensated by the development of a fine vascular network that resembles "puffs of smoke" ("moyamoya" in Japanese).[12,13] Moyamoya disease occurs with the highest prevalences in East Asian countries such as Japan, Korea, and China, especially compared with other countries worldwide.[2,7,10]

We previously identified a susceptibility locus for familial moyamoya disease on 17q25.3.[11] Significant associations with genes in this region had been reported,[4,8] but rigorous identification had not been

determined. The *ring finger 213 (RNF213)* gene was finally identified as a susceptibility gene for moyamoya disease by the conventional rigorous positional cloning approach, exome analysis, and functional analysis using zebrafish.[9] Overall, 74.5% of East Asian patients with moyamoya disease carry the rare founder variant p.R4810K of *RNF213*. However, a gradient of prevalence was observed in patients with moyamoya disease: 90% in Japanese, 79% in Korean, and 23% in Chinese patient populations. On the other hand, no gradient of prevalence was observed in these three general populations. In total, 2.4% of the East Asian general population carries p.R4810K. The minor allele frequencies of p.R4810K were 1.4%, 1.3%, and 1.0% for the Japanese, Korean, and Chinese in general populations, respectively.[9] These similar allele frequencies of p.R4810K in these three East Asian general populations do not explain the lower frequency of Chinese patients with moyamoya disease compared with Japanese and Korean patients with moyamoya

disease. Moyamoya disease occurs in approximately one of 300 carriers in Japan.[8] This discrepancy in the allele frequency between cases and controls in Chinese people might be attributable to selection bias in the general populations in the previous study.[9]

The primary aim of the present study was to estimate the population susceptible to moyamoya disease by conducting large scale screening for p.R4810K in general populations in East and Southeast Asia. The secondary aim was to estimate association of the p.R4810K variant of RNF213 in patients with moyamoya disease.

Materials and Methods

A total of 2,508 unrelated participants from East Asian and Southeast Asian countries were recruited, comprising 587 Chinese, 294 Korean, 1474 Japanese, 103 Vietnamese, and 50 Filipino people (Table 1). The Japanese participants were recruited from mainland Japan, including Hokkaido, Honshu, Shikoku, and Kyushu, and Okinawa. The Korean participants were recruited from five locations. The Chinese participants were recruited from 11 loca-

tions. Blood samples were obtained from two sources. One source was the Kyoto University Human Specimen Bank, which collected blood samples from the 1990s and 2000s as previously described.[5,6] These blood samples included Chinese, Korean, Japanese, and Philippine samples. The other source involved samples collected in an international collaboration that included Vietnam and Seoul, South Korea.

Ethical approval for this study was given by the Institutional Review Board and Ethics Committee of Kyoto University School of Medicine, Kyoto University, Japan (approval number: G140; approval date: Oct. 18, 2004), by the Institutional Review Board of Seoul National University Hospital, Seoul, South Korea (approval number: H0507-509-153; approval date: Aug. 24, 2005). The study participants were recruited in these institutes. Subjects who participated in this study after 2000 were recruited by School of Medicine, Kyoto University. All subjects gave written informed consent. Subjects who donated blood samples before 2000 were recruited by Tohoku University School of Medicine (Sendai, Miyagi), or Akita University School of Medicine (Akita, Akita), or Kyoto University School of Medicine, and

Table 1 Demographic features of the participants in the East and Southeast Asian populations

Area	Country	Location	Size of population (million)	Sex (male:female)	Age (yrs)*	Angiography**
East Asia	China	Dehui	1.00	0:50	NA	0
		Huludao	2.82	0:50	NA	0
		Beijing	19.61	0:50	38.4 ± 10.6	0
		Jinan	6.81	0:50	NA	0
		Xian	8.47	0:94	NA	0
		Baoji	3.72	0:48	NA	0
		Shanghai	23.02	0:50	NA	0
		Changsha	7.04	0:50	NA	0
		Heping	4.60	0:46	NA	0
		Nanning	6.66	0:50	NA	0
		Tainan	1.88	0:49	36.4 ± 11.5	0
		Total	85.63	0:587	37.4 ± 11.1	0
	Korea	Seoul	10.46	80:25	42.2 ± 13.3	46
		Chonan	0.58	0:29	34.6 ± 8.8	0
		Haman	0.06	0:46	43.6 ± 6.8	0
		Pusan	3.60	0:49	39.4 ± 7.8	0
		Jeju-do	0.53	0:65	NA	0
		Total	15.23	80:214	40.9 ± 10.9	46
	Japan	Mainland	123.62	608:766	57.7 ± 14.1	384
		Okinawa	1.38	0:100	47.5 ± 7.2	0
		Total	125.00	608:866	57.0 ± 14.0	384
Southeast Asia	Vietnam	Hanoi	6.50	0:103	22.8 ± 10.2	0
	Philippines	Manila	1.66	0:50	NA	0

*Values are means ± standard deviation. **Conventional digital subtraction angiography, magnetic resonance angiography, computed tomography angiography, and others. NA: not applicable.

gave verbal informed consent. The use of blood samples donated before 2000 for genetic analysis was also approved by the Institutional Review Board and Ethics Committee of Kyoto University School of Medicine (approval number: G140; approval date: Oct. 18, 2004).

Peripheral blood (10 ml) was collected from all participants. Genomic deoxyribonucleic acid (DNA) was extracted from the blood samples using a QIAamp DNA Blood Mini Kit (Qiagen, Germantown, Maryland, USA) according to the manufacturer's protocol. The quality and concentration of the extracted DNA were assessed using an Infinite® M200 PRO (TECAN, Kawasaki, Kanagawa). The DNA was stored in a freezer at −20°C until analysis.

Genotyping of p.R4810K in all participants was conducted using a TaqMan® probe (Custom TaqMan® SNP Genotyping Assays; Applied Biosystems, Foster City, CA, USA) and a 7300/7500 Real-Time PCR System (Applied Biosystems) according to the manufacturer's protocols. Briefly, the polymerase chain reaction (PCR) amplifications were performed with 1–20 ng of purified genomic DNA, 0.1 μl of 40× SNP Genotyping Assay, 6.25 μl of 2× TaqMan® Universal PCR Master Mix, No

AmpErase® UNG, and 5.15 μl of deoxyribonuclease-free water. The final reaction volume was 12.5 μl/well in 96-well plates. The standard protocol for the cycling conditions was maintenance for 10 minutes at 95°C for AmpliTaq Gold® (Applied Biosystems) enzyme activation, followed by 40 cycles of 15 seconds at 92°C for denaturation, and 1 minute at 60°C for annealing/extension. After each PCR amplification, an endpoint plate read was performed using the Real-Time PCR System (Applied Biosystems). The associated sequence detection system software uses the fluorescence measurements taken during the plate read to plot fluorescence (normalized reporter signal: Rn) values based on the signals from each well. The plotted fluorescence signals indicate which alleles are present in each sample.

Results

The demographic features of all participants in this study are shown in Table 1. The sampled cities covered 234.02 million people. A total of 2,508 participants from three East Asian countries and two Southeast Asian countries were recruited from 1987

Table 2 Geographic distribution of p.R4810K in *RNF213* in East and Southeast Asian populations

Area	Country	Location	Genotype of p.R4810K			Sample size	Minor allele frequency (%)	Total population (million)	Estimated population with p.R4810K in a country (million)
			GG	GA	AA				
East Asia	China	Dehui	50	0	0	50	0.00		
		Huludao	50	0	0	50	0.00		
		Beijing	49	1	0	50	1.00		
		Jinan	50	0	0	50	0.00		
		Xian	92	2	0	94	1.06		
		Baoji	48	0	0	48	0.00	1340.00	11.41
		Shanghai	49	1	0	50	1.00		
		Changsha	50	0	0	50	0.00		
		Heping	46	0	0	46	0.00		
		Nanning	49	1	0	50	1.00		
		Tainan	49	0	0	49	0.00		
		Total	582	5	0	587	0.43		
	Korea	Seoul	102	3	0	105	1.43		
		Chonan	28	1	0	29	1.72		
		Haman	45	1	0	46	1.09	50.00	1.36
		Pusan	48	1	0	49	1.02		
		Jeju-do	63	2	0	65	1.54		
		Total	286	8	0	294	1.36		
	Japan	Mainland	1339	32	3	1374	1.38		
		Okinawa	98	2	0	100	1.00	125.00	3.39
		Total	1437	34	3	1474	1.36		
Southeast Asia	Vietnam	Hanoi	103	0	0	103	0.00	90.50	0.00
	Philippines	Manila	50	0	0	50	0.00	94.00	0.00

Fig. 1 Locations of the sampling sites in East and Southeast Asian countries.

to 2009. Briefly, the recruited subjects comprised 587 participants from 11 Chinese locations, 294 from five Korean locations, 1474 from five Japanese locations, 103 from one Vietnamese location, and 50 from one Philippines location. Most of the participants were females, with the exception of 608 Japanese males and 80 Korean males. Information on age was only available for the participants from certain locations. Angiography was only conducted for 384 Japanese and 46 Korean participants.

The geographic distributions of p.R4810K in the different ethnicities are shown in Table 2 and Fig. 1. p.R4810K was detected in East Asian populations, but not in Southeast Asian populations. p.R4810K was detected at allele frequencies of 0.43%, 1.36%, and 1.36% in the Chinese, Korean, and Japanese populations, respectively. p.R4810K was detected at an allele frequency of about 1.00% in 4 of 11 investigated locations in China, suggesting that the distribution of p.R4810K was heterogeneous and limited to certain specific locations in China. In contrast, p.R4810K was homogeneously located throughout Korea and Japan at relatively high allele frequencies of 1.00–1.72%. p.R4810K was not detected in 49 Taiwanese, 103 Vietnamese, and 50 Filipino participants.

Discussion

The present study confirmed the presence of similar allele frequencies of the variant p.R4810K of *RNF213* in the Japanese and Korean general populations. However, expansion of the examined population revealed that the allele frequency of p.R4810K in the Chinese population was 0.43%, only one-third of the

frequency in the Japanese or Korean populations. Therefore, our previous observation was considered to be attributable to selection bias.[9] The lower prevalence of p.R4810K in the Chinese general population might be proportional to the lower carrier rate (i.e., 23%) in Chinese patients. In accordance with this observation, a single dominant polymorphism may be associated with Japanese or Korean patients, whereas various polymorphisms in *RNF213* may be associated with Chinese patients. In fact, we observed five additional mutations in Chinese patients but no additional mutations in Korean or Japanese patients.[9]

In the present study, magnetic resonance angiography was only conducted for limited numbers of participants. This limitation did not affect our results because of the very low prevalences of moyamoya disease in the general populations. The estimated total numbers of carriers were 11.41 million for the Chinese, 1.36 million for the Korean, and 3.39 million for the Japanese populations. Assuming that moyamoya disease occurs in one of 300 carriers with p.R4810K,[8,9] the estimated numbers of patients with moyamoya disease attributable to p.R4810K are 38,000 in the Chinese, 4,500 in the Korean, and 11,300 in the Japanese populations. Although these numbers are very approximate and minimum estimates, because only the p.R4810K variant is considered, the large number of potential sufferers suggests that more attention should be paid to moyamoya disease in East Asian countries.

Differences in the clinical profiles of moyamoya disease have been recognized in China, Korea, and Japan.[1,3] However, the differences between the clinical profiles of Korean and Japanese patients are unlikely to be explained by genetic differences. Specific factor(s) other than the genetic factor are needed to explain the variations in the clinical phenotypes and low penetrance among carriers.[8,9] Therefore, unknown modifier factor(s) may also be contributory to the differences in the clinical phenotypes. Further research is needed to identify such factor(s), which may also be crucial for the development of moyamoya disease among carriers of variant p.R4810K in *RNF213*.

Acknowledgments

young scientists.

References

1) Duan L, Bao XY, Yang WZ, Shi WC, Li DS, Zhang ZS, Zong R, Han C, Zhao F, Feng J: Moyamoya disease in China: its clinical features and outcomes. *Stroke* 43: 56–60, 2012

2) Goto Y, Yonekawa Y: Worldwide distribution of moyamoya disease. *Neurol Med Chir (Tokyo)* 32: 883–886, 1992

3) Ikezaki K, Han DH, Kawano T, Kinukawa N, Fukui M: A clinical comparison of definite moyamoya disease between South Korea and Japan. *Stroke* 28: 2513–2517, 1997

4) Kamada F, Aoki Y, Narisawa A, Abe Y, Komatsuzaki S, Kikuchi A, Kanno J, Niihori T, Ono M, Ishii N, Owada Y, Fujimura M, Mashimo Y, Suzuki Y, Hata A, Tsuchiya S, Tominaga T, Matsubara Y, Kure S: A genome-wide association study identifies RNF213 as the first Moyamoya disease gene. *J Hum Genet* 56: 34–40, 2011

5) Koizumi A, Harada KH, Inoue K, Hitomi T, Yang HR, Moon CS, Wang P, Hung NN, Watanabe T, Shimbo S, Ikeda M: Past, present, and future of environmental specimen banks. *Environ Health Prev Med* 14: 307–318, 2009

6) Koizumi A, Yoshinaga T, Harada K, Inoue K, Morikawa A, Muroi J, Inoue S, Eslami B, Fujii S, Fujimine Y, Hachiya N, Koda S, Kusaka Y, Murata K, Nakatsuka H, Omae K, Saito N, Shimbo S, Takenaka K, Takeshita T, Todoriki H, Wada Y, Watanabe T, Ikeda M: Assessment of human exposure to polychlorinated biphenyls and polybrominated diphenyl ethers in Japan using archived samples from the early 1980s and mid-1990s. *Environ Res* 99: 31–39, 2005

7) Kuroda S, Houkin K: Moyamoya disease: current concepts and future perspectives. *Lancet Neurol* 7: 1056–1066, 2008

8) Liu W, Hashikata H, Inoue K, Matsuura N, Mineharu Y, Kobayashi H, Kikuta KI, Takagi Y, Hitomi T, Krischek B, Zou LP, Fang F, Herzig R, Kim JE, Kang HS, Oh CW, Tregouet DA, Hashimoto N, Koizumi A: A rare Asian founder polymorphism of Raptor may explain the high prevalence of Moyamoya disease among East Asians and its low prevalence among Caucasians. *Environ Health Prev Med* 15: 94–104, 2010

9) Liu W, Morito D, Takashima S, Mineharu Y, Kobayashi H, Hitomi T, Hashikata H, Matsuura N, Yamazaki S, Toyoda A, Kikuta K, Takagi Y, Harada KH, Fujiyama A, Herzig R, Krischek B, Zou L, Kim JE, Kitakaze M, Miyamoto S, Nagata K, Hashimoto N, Koizumi A: Identification of RNF213 as a susceptibility gene for moyamoya disease and its possible role in vascular development. *PLoS One* 6: e22542, 2011

10) Miao W, Zhao PL, Zhang YS, Liu HY, Chang Y, Ma J, Huang QJ, Lou ZX: Epidemiological and clinical features of Moyamoya disease in Nanjing, China. *Clin Neurol Neurosurg* 112: 199–203, 2010

11) Mineharu Y, Liu W, Inoue K, Matsuura N, Inoue S, Takenaka K, Ikeda H, Houkin K, Takagi Y, Kikuta K, Nozaki K, Hashimoto N, Koizumi A: Autosomal dominant moyamoya disease maps to chromosome 17q25.3. *Neurology* 70: 2357–2363, 2008

12) Suzuki J, Takaku A: Cerebrovascular "moyamoya" disease. Disease showing abnormal net-like vessels in base of brain. *Arch Neurol* 20: 288–299, 1969

13) Takeuchi K, Shimizu K: [Hypogenesis of bilateral internal carotid arteries]. *No To Shinkei* 9: 37–43, 1957 (Japanese)

Address reprint requests to: Akio Koizumi, MD, Department of Health and Environmental Sciences, Graduate School of Medicine Kyoto University, Konoe-cho, Yoshida, Sakyo-ku, Kyoto 606-8501, Japan.
e-mail: koizumi.akio.5v@kyoto-u.ac.jp

PLoS one

Identification of *RNF213* as a Susceptibility Gene for Moyamoya Disease and Its Possible Role in Vascular Development

Wanyang Liu[1◉], Daisuke Morito[2◉], Seiji Takashima[3◉], Yohei Mineharu[4◉], Hatasu Kobayashi[1◉], Toshiaki Hitomi[1◉], Hirokuni Hashikata[1,4◉], Norio Matsuura[1◉], Satoru Yamazaki[5], Atsushi Toyoda[6], Ken-ichiro Kikuta[4], Yasushi Takagi[4], Kouji H. Harada[1], Asao Fujiyama[6,7], Roman Herzig[8], Boris Krischek[9], Liping Zou[10], Jeong Eun Kim[11], Masafumi Kitakaze[5], Susumu Miyamoto[4], Kazuhiro Nagata[2], Nobuo Hashimoto[4,5]*, Akio Koizumi[1]*

1 Department of Health and Environmental Sciences, Kyoto University, Kyoto, Japan, 2 Faculty of Life Sciences, Kyoto Sangyo University, Kyoto, Japan, 3 Department of Molecular Cardiology, Osaka University, Suita, Osaka, Japan, 4 Department of Neurosurgery, Kyoto University, Kyoto, Japan, 5 National Cerebral and Cardiovascular Center, Suita, Osaka, Japan, 6 Comparative Genomics Laboratory, National Institute of Genetics, Mishima, Shizuoka, Japan, 7 Principles of Informatics Research Division, National Institute of Informatics, Tokyo, Japan, 8 Palacky University Hospital, Olomouc, Czech Republic, 9 Department of Neurosurgery, University of Tubingen, Tubingen, Germany, 10 Department of Pediatrics, Chinese People's Liberation Army General Hospital, Beijing, People's Republic of China, 11 Seoul National University College of Medicine, Seoul, Korea

Abstract

Background: Moyamoya disease is an idiopathic vascular disorder of intracranial arteries. Its susceptibility locus has been mapped to 17q25.3 in Japanese families, but the susceptibility gene is unknown.

Methodology/Principal Findings: Genome-wide linkage analysis in eight three-generation families with moyamoya disease revealed linkage to 17q25.3 ($P<10^{-4}$). Fine mapping demonstrated a 1.5-Mb disease locus bounded by D17S1806 and rs2280147. We conducted exome analysis of the eight index cases in these families, with results filtered through Ng criteria. There was a variant of p.N321S in *PCMTD1* and p.R4810K in *RNF213* in the 1.5-Mb locus of the eight index cases. The p.N321S variant in *PCMTD1* could not be confirmed by the Sanger method. Sequencing *RNF213* in 42 index cases confirmed p.R4810K and revealed it to be the only unregistered variant. Genotyping 39 SNPs around *RNF213* revealed a founder haplotype transmitted in 42 families. Sequencing the 260-kb region covering the founder haplotype in one index case did not show any coding variants except p.R4810K. A case-control study demonstrated strong association of p.R4810K with moyamoya disease in East Asian populations (251 cases and 707 controls) with an odds ratio of 111.8 ($P=10^{-119}$). Sequencing of *RNF213* in East Asian cases revealed additional novel variants: p.D4863N, p.E4950D, p.A5021V, p.D5160E, and p.E5176G. Among Caucasian cases, variants p.N3962D, p.D4013N, p.R4062Q and p.P4608S were identified. *RNF213* encodes a 591-kDa cytosolic protein that possesses two functional domains: a Walker motif and a RING finger domain. These exhibit ATPase and ubiquitin ligase activities. Although the mutant alleles (p.R4810K or p.D4013N in the RING domain) did not affect transcription levels or ubiquitination activity, knockdown of *RNF213* in zebrafish caused irregular wall formation in trunk arteries and abnormal sprouting vessels.

Conclusions/Significance: We provide evidence suggesting, for the first time, the involvement of *RNF213* in genetic susceptibility to moyamoya disease.

Introduction

Moyamoya disease is an idiopathic disorder characterized by occlusive lesions in the supraclinoid internal carotid artery and its main branches in the circle of Willis. To compensate for the blood flow around the occlusive region, a fine vascular network develops that resembles "puffs of smoke" (Figure 1A) [1]. The unique appearance of moyamoya vessels described by Suzuki and Takaku
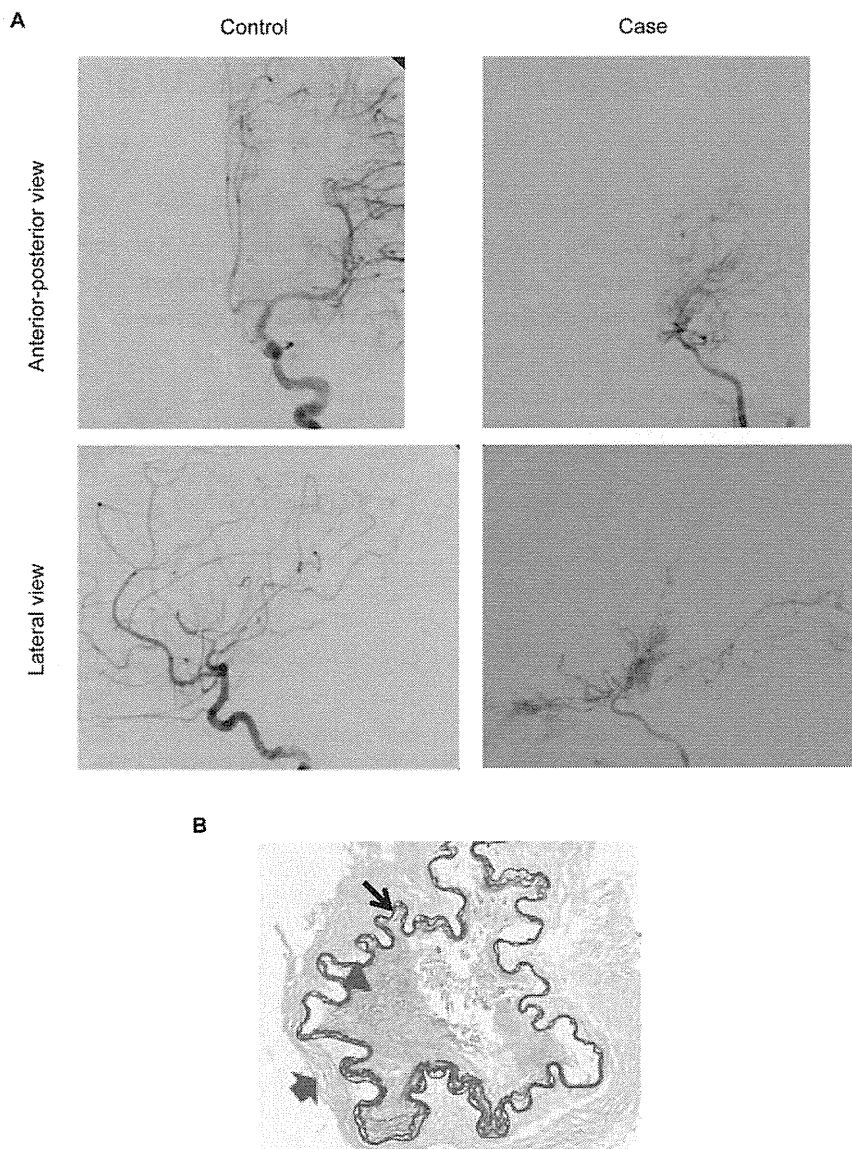
93

Figure 1. Clinical features of moyamoya disease. (**A**) An anterior-posterior and lateral views of left internal carotid angiography in a 9-year-old child with moyamoya disease (right) and an 8-year-old control child (left). An occlusion with moyamoya vessels can be seen around the terminal portion of the internal carotid artery and proximal portions of the anterior cerebral artery and middle cerebral artery in the affected child. (**B**) Intimal hyperplasia in the middle cerebral artery from an autopsy of a 69-year-old case. Intimal hyperplasia (red arrowhead), atrophic media (red arrow) and winding internal elastic lamina (black arrow) can be seen with Elastica Masson staining, ×200.
doi:10.1371/journal.pone.0022542.g001

in 1969 [2] spurred international recognition of moyamoya disease [MIM 607151] (Online Mendelian Inheritance in Man in Appendix S1). Moyamoya disease occurs worldwide [3], but its prevalence is highest in East Asian countries, including Japan (1 in 10,000), Korea and China [4], [5]. It is known to cause stroke in neonates and children, and therefore pathological clues for early diagnosis and novel therapeutic approaches are needed [6].

The occlusive lesions are caused by excessive proliferation of smooth muscle cells (SMCs), which specifically occurs in arteries in the skull with compensatory bypass vessels (Figure 1B) [7]. These occlusive lesions are similar to those of atherosclerosis in that both types of lesion exhibit endothelial injury, SMC proliferation and intimal hyperplasia. However, there are major differences between the two types: in moyamoya vessels, infiltrating cellular components such as macrophages and lipid deposits are not observed [8].

A recent study revealed that accelerated vascular remodeling might underlie the pathological consequences of moyamoya disease [9]. Clinical investigations have revealed elevated levels of certain growth factors or cytokines in the cerebrospinal fluid, serum or blood vessels of patients with moyamoya disease [10]–[15]. These factors are assumed to be associated with vascular remodeling.

Epidemiological studies have revealed several risk factors associated with moyamoya disease, including Asian ethnicity, female gender and a family history of the disease [4]. Given that 15% of moyamoya patients have a family history of the disease, genetic factors are suspected to underlie its pathogenesis.

Several studies have explored genetic factors and revealed four loci associated with moyamoya disease: 3p24–p26 [16], 6q25 [17], 8q23 [18] and 17q25 [19]. The locus on 17q25, first mapped by

94

Yamauchi *et al.* [19], was replicated in 2008 [20], [21]. In our previous study, a strong association of a variant (ss161110142) was demonstrated in East Asian patients, suggesting a possible East Asian founder haplotype for moyamoya disease [21]. The major aim of the present study was to identify the causative gene for moyamoya disease. In the present study, we conducted exome analysis and identified ring finger protein 213 (*RNF213*; DDBJ/EMBL/GenBank accession number AB537889) [National Center for Biotechnology Information (NCBI) in Appendix S1] as a susceptibility gene. In this study, we cloned *RNF213* and determined its open reading frame (ORF). Compared with the previously registered *RNF213* sequence [NM_020914.4] (NCBI in Appendix S1), our *RNF213* clone possesses a 2,500-bp longer 3′ untranslated region (UTR) and lacks exon 4. Since we found that AB537889 seems to be the major transcript of *RNF213*, the descriptions of *RNF213* in this paper are primarily based on the newly determined ORF unless otherwise stated.

Methods

Ethical statement

Ethical approval for this study was given by the Institutional Review Board and Ethics Committee of Kyoto University School of Medicine, Kyoto University, Japan (approval number: G140; approval date: 10/18/2004); by the Ethics Committee of the medical faculty of the University of Tübingen (Ethik-Kommission der Medizinischen Fakultät des Universitätsklinikums Tübingen; permit number: 273/2009BO1; approval date: 1/1/2009); by Seoul National University Hospital Institutional Review Board (approval number: H0507-509-153; approval date 8/24/2005); by the Medical Ethics Committee of Beijing Children's Hospital Institutional Review Board, Capital Medical University, China (approval number: 2005-31; approval date: 3/15/2005); and by the Ethics Committee of University Hospital and the Faculty of Medicine of Palacky University in Olomouc (reference number: 62/10; approval date: 8/18/2008). Participants were recruited in these institutes. All subjects gave written informed consent, or for those considered too young to consent, informed consent was given by their parent or guardian.

Subjects

Diagnostic criteria were based on the Japanese Research Committee on moyamoya disease of the Ministry of Health, Welfare and Labour, Japan (RCMJ) criteria [22]. Information on family histories, gender, age of onset, onset of symptoms and unilateral or bilateral moyamoya disease was obtained either by interview or by clinical chart review, as previously reported [21], [23].

We recruited East Asian cases (Japanese, Korean and Chinese), as described previously [21]. The participants comprised 41 Japanese families and one Korean family (Figure S1 and Table S1), 209 unrelated cases (120 Japanese, 37 Korean and 52 Chinese). We recruited 757 unrelated controls: 384 Japanese, 223 Korean and 100 Chinese (Table S2) and an additional 50 Chinese adult females [Mean age at participation (years ± SD): 38.4±10.5].

We also recruited a Caucasian family of Czech ethnicity (Figure S2A) and 7 unrelated Czech and 42 German cases with moyamoya disease at the University of Tubingen (Germany), and Palacky University and University Hospital (Olomouc, Czech Republic). The mean age (years ± SD) at diagnosis was 30.4±14.7, and the sex ratio of males:females was 16:33. The 284 Caucasian controls were recruited from Palacky University and University Hospital ($n = 120$), the University of Tubingen

($n = 164$) and another 100 Caucasian control samples (the Coriell Caucasian Panel) were bought from the Coriell Institute. The mean age (years ± SD) was 43.9±17.9 and the sex ratio of males:females was 176:208. No magnetic resonance imaging screening of the controls was conducted.

Linkage, haplotype and segregation analyses

We conducted a parametric genome-wide linkage analysis using GENEHUNTER [24] (GENEHUNTER Ver2.1_r6: Appendix S1) in the eight largest three-generation families (peds. 2, 10, 14, 15, 17–20) (Figure 2) with an ABI Prism Linkage Mapping Set (Version 2; Applied Biosystems) with 382 markers, 10 cM apart, for 22 autosomes, and fine-mapping markers designed according to information from the uniSTS reference physical map (http://www.ncbi.nlm.nih.gov/genome/sts/). Unaffected members were treated as "phenotype unknown" because of the incomplete and age-dependent penetrance of moyamoya disease [20]. We considered obligate carriers and subjects with unilateral occlusion or stenosis around the circle of Willis as affected, as previously reported [20]. The disease allele frequency was set at 0.00002 and a phenocopy frequency of 0.000001 was assumed, as previously reported [20]. Population allele frequencies were assigned equal portions for individual alleles. We performed multipoint analyses for autosomes and obtained logarithm of the odds (LOD) scores. Haplotypes were constructed with GENEHUNTER and segregation was investigated using the constructed haplotypes.

To calculate the statistical significance level of the linkage to 17q25.3 in the eight families, we applied a bootstrap method using simulation, as previously reported [25]. We simulated recombination events for 22 chromosomes in these eight families, calculated multipoint LOD scores by GENEHUNTER and obtained the maximum total LOD scores in each trial. The simulation was run 10,000 times.

Exome analysis

We conducted exome analysis on one index case from each of the eight families (peds. 2, 10, 14, 15, 17–20) (Figure 2), who were diagnosed with moyamoya disease based on RCMJ criteria. We targeted all protein-coding regions as defined by RefSeq37 (RefSeq in Appendix S1). Approximately 210,121 coding exons in the 20,794 target genes from 10μg of genomic DNA from each case were captured using an Agilent SureSelect Human All Exon kit, following the manufacturer's protocols. Briefly, DNA was sheared by acoustic fragmentation (Covaris) and purified using a QIAquick PCR Purification kit (Qiagen). The quality of the fragmentation and purification was assessed with an Agilent 2100 Bioanalyzer. The fragment ends were repaired and adaptors were ligated to them (NEBNext DNA sample prep; New England Biolabs). The resulting DNA library was purified using a QIAquick PCR Purification kit, amplified by PCR and captured by hybridization to the biotinylated RNA library "baits" (Agilent). The whole-exome DNA library was sequenced on an Illumina Genome Analyzer IIx in 76-bp paired-end reads using two channels. Sequence reads were mapped to the reference human genome (Ghr37/hg19) (NCBI and UCSC Genome Browser in Appendix S1) using ELANDv2 software (Illumina). Variant detection was performed with CASAVA software (version 1.7; Illumina). Sequence calls were filtered to include only those with >8 coverage, >30 consensus quality and >20 mapping quality. Candidate variants were filtered by SAMtools (Appendix S1). For comparison, we used an exome database of five Japanese controls, who do not have histories of stroke, for which the analysis was conducted by the same protocol and experimental procedures.
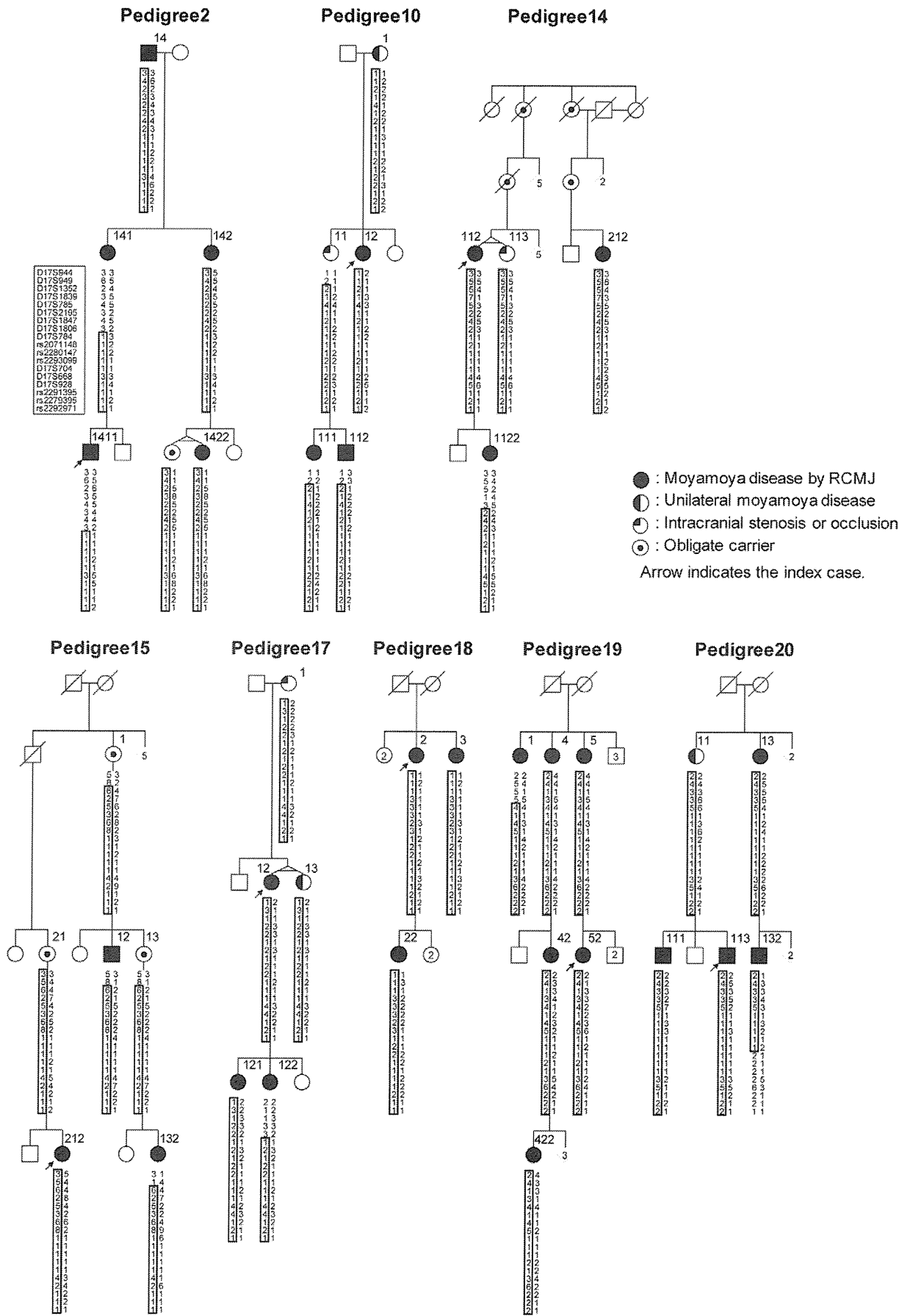
95

● : Moyamoya disease by RCMJ
◑ : Unilateral moyamoya disease
◓ : Intracranial stenosis or occlusion
⊙ : Obligate carrier
Arrow indicates the index case.

Figure 2. The eight three-generation families and haplotype construction with fine markers. For familial index cases in the eight pedigrees, the haplotypes are indicated by the boxes constructed in GENEHUNTER [24]. The smallest disease haplotype spanning from D17S1806 to rs2280147 was estimated by the region common to both 1411 in the pedigree 2 and 132 in pedigree 20.
doi:10.1371/journal.pone.0022542.g002

Direct sequencing of *RNF213* and *PCMTD1* by the Sanger method

Genomic DNA was extracted from blood samples with a QIAamp DNA Blood Mini kit (Qiagen). The whole *RNF213* gene was sequenced, including the 5′ promoter region at least 2 kb upstream of the first exon, 50–300 bp of each intron upstream and downstream of each exon, all the exons and throughout the 3′ UTR. Target sequences, including the skipped exon 4 were based on the open reading frame of NM_020914.4. Sequencing exon 8 of *PCTDM1* was conducted to confirm the exome result. Sequencing primers were commercially synthesized (PROLIGO Primers & Probes) (Table S3) (Appendix S1). The PCR products were separated on an ABI Prism 3130 Avant DNA sequencer (Applied Biosystems, Tokyo, Japan).

Deep sequencing of introns and intergenic regions of *RNF213*

To search for a hidden causative variant, we sequenced the entire 260-kb genomic region from the 5′ end of *SLC26A11* (bp 78194200) to the 5′ end of *NPTX1* (bp 78450404) (NCBI in Appendix S1) in the index case of pedigree 11, who was homozygous at 17q25.3 because of parental consanguineous marriage, using two bacterial artificial chromosome (BAC) clones (bp 78194200–78238718 and bp 78345170–78450404) (Table S4) or by direct sequencing. The entire RNF213 gene including promoters, 5′UTR, introns, exons and 3′UTR was sequenced in a control sample in the same way as for the index case of pedigree 11. Since we failed to sequence intron 15 of *RNF213*, we used Southern blotting to detect a possible expansion. Details of the BAC cloning and Southern blotting are described in the Text S1. The primer sequences are listed in Table S3.

Genotyping of five rare variants (ss179362671, ss179362673 (p.R4810K), ss179362674, ss179362675 ss161110142) and 34 other single nucleotide polymorphisms (SNPs)

Typing of the five rare variants and 34 SNPs was conducted using Taqman probes (TaqMan SNP Genotyping Assays; Applied Biosystems) using a 7300/7500 Real-Time PCR System (Applied Biosystems) (dbSNP 131 and Hapmap database in Appendix S1). The transmitted haplotypes in 42 families were constructed using GENEHUNTER. Details of the 39 SNPs are described in the Text S1. The allele frequencies were determined in Japanese controls.

Copy number variations (CNVs)

We performed genotyping with Affymetrix 500K arrays (GeneChip® Mapping 250/500 K; Affymetrix, Inc.) according to the manufacturer's protocol. Genomic DNA samples donated by the index cases of pedigrees 5, 11 and 18 and the control spouse of 2 of pedigree 18 were analyzed. The genome-wide call rates were >95% for all the genomic DNAs. CNVs were identified from the intensities using the Affymetrix GeneChip® Chromosome Copy Number Analysis Tool software V.4.01. CNVs were observed using CNAG viewer (Version 2.0; Takara).

Association study with p.R4810K (ss179362673)

Association studies were conducted between 161 Japanese cases (41 index cases from Japanese families and unrelated 120 cases) and 384 Japanese controls, between 38 Korean cases (the index case from a Korean family and 37 cases) and 223 Korean controls and between 52 Chinese cases and 100 Chinese controls (Tables S1 and S2). Cases were exclusively diagnosed as moyamoya by RCMJ criteria.

The association was investigated using SNP & Variation Suite V7 (Golden Helix, Inc. in Appendix S1). Allelic, additive, dominant and recessive models were tested. Population-attributable risk (PAR) was defined as PAR $= 100*(K-y)/K$, where K is the population prevalence and y is the phenocopy proportion that was estimated from the number of cases with the risk allele [21].

Screening of *RNF213* polymorphisms in controls

Five *RNF213* variants, p.D4863N, p.E4950D, p.A5021V, p.D5160E and p.E5176G were screened in 757 East Asian controls: 384 Japanese, 223 Korean, and 150 Chinese. Four variants, p.N3962D, p.D4013N, p.R4062Q and p.P4608S, were screened in 384 Caucasian controls: 120 Czech, 164 German, and 100 Caucasian. The screening methods were described in the Text S1 and in Table S5.

Immortalized cell lines, cell culture and transient transfection

Lymphoblastoid cell lines (LCLs) were isolated and immortalized with Epstein-Barr virus for five unrelated controls (three individuals, the spouse of individual 2 in pedigree 18 and the spouse of individual 12 in pedigree 17) and six cases (individuals 2 and 22 in pedigree 18, individual 11 in pedigree 11 and individuals 12, 121 and 122 in pedigree 17). HeLa cells and human embryonic kidney (HEK) 293 cells were cultured in Dulbecco's modified Eagle's medium (Invitrogen) supplemented with 10% fetal bovine serum. Human umbilical vein endothelial cells (HUVECs) and coronary artery smooth muscle cells (CASMCs) were grown in EBM-2 and SmBM-2 (Lonza), respectively. Expression plasmids were transfected into cells using Lipofectamine LTX (Invitrogen) in accordance with the manufacturer's instructions.

Cloning of *RNF213* and construction of an expression vector

We cloned *RNF213* and constructed wild-type and various mutants of the *RNF213* expression vector as described in the Text S1. Nucleotide sequence data reported are available in the DDBJ/EMBL/GenBank databases under the accession number AB537889 (NCBI in Appendix S1).

Detection of splicing products of *RNF213* cDNA or *FLJ35220* cDNA and real-time quantitative PCR

A Human Total RNA Master Panel II (Clontech Inc) and total RNA from the Artery (BioChain) were reverse-transcribed into cDNA using the High Capacity cDNA Reverse Transcription kit (Applied Biosystems). We tested whether *RNF213* cDNA skipped exon 4 of *RNF213* by molecular sizing and direct sequencing of cDNA isolated from the RNA of the above human tissues, HUVECs, and LCLs isolated from the five controls and six cases. The PCR primers were designed to cover exons 3–5 as described in the Text S1. We also tested whether or not *FLJ35220* cDNA skipped exon 11 of *FLJ35220* due to G>A substitution in the

97